Journal of Applied Polymer Science

Layered Double Hydroxide Platelets Exfoliation Into a Water-Based Polyester

C.H. Swanson,[1] T. Stimpfling,[1] A.-L. Troutier-Thulliez,[1] H. Hintze-Bruening,[2] F. Leroux[1]

[1]Institut de Chimie de Clermont-Ferrand (ICCF), Clermont Université, Université Blaise Pascal, CNRS, UMR 6096, F-63177 Aubière, France

[2]BASF Coatings GmbH, Glasuritstrasse 1, 48165 Muenster, Germany

Correspondence to: F. Leroux (E-mail: fabrice.leroux@univ-bpclermont.fr)

ABSTRACT: Nitrate layered double hydroxide (LDH) phase $Zn_2Al(OH)_6(NO_3)\cdot 2H_2O$ is successfully exfoliated in the presence of polyester under mild conditions using water as essential solvent and at room temperature under air. From small angle X-ray scattering spectroscopy a total exfoliation is found to be achieved using up to 10 wt % LDH, while intercalated polymer nanocomposite structures largely extended up to 14 nm are observed for loading ranging from 10 to 20 wt %. The process is found to be explained by the diffusion of the polymer chain into the interlayer host structure. Starting from an initial value of 0.89 nm, ≈3, 7, 10, 14, and 20 nm transient interleaved nanostructures are formed without any carbonate uptake. The collective gap distance is certainly due to a defined number of polymer chains diffusing into the LDH interstices. Similarly, starting from an aqueous polyester solution highly concentrated in LDH nitrate phase up to 50% w.w, successive dilutions yield platelet exfoliation, thus rendering a smooth chemistry process attractive for potential applications. © 2012 Wiley Periodicals, Inc. J. Appl. Polym. Sci. 000: 000–000, 2012

KEYWORDS: clay; colloids; light scattering; polyesters; X-ray

Received 30 May 2012; accepted 3 August 2012; published online
DOI: 10.1002/app.38483

INTRODUCTION

A straightforward and scalable process to exfoliate inorganic platelets has been in the focus of many studies from the materials science community and in particular for those devoted to polymer nanocomposite to fulfill in particular properties related to mechanical reinforcement and barrier properties.[1–4] It requires a modification of the platelets surface by organic molecules, generally long alkyl chain surfactant molecule,[5,6] in order to compatibilize them with the polymer chains and to promote the diffusion of the latter into the interlayer spacing. Subsequent exfoliation in most cases requires shearing forces helping to disagglomerate the hybrid structure during the polymer nanocomposite preparation. Such a multiple step process is energy-demanding, molecular inefficient and in many cases questionable in view of scalability.

We focus our study on the exfoliation of layered double hydroxide (LDH) into a waterborne polyester dispersion using a simple procedure.

Polyesters as a class of polymer receive a lot of attention due to its compatibility with other polymers and biopolymers[7] as well as being biodegradable in some cases.[8–10] Additionally, a number of monomeric diols and diacids, like fatty acid derivatives, can be biobased.[11–13] Therefore, many efforts have been undertaken to promote their properties and in particular the barrier properties (water, fire) through the nanocomposite approach.[14–16] Indeed other barrier and mechanical properties regarding stone-chip resistance in automotive coatings were recently found to be enhanced for polyester-based polyurethane formulations using LDH platelets.[17–19] LDH-type material structure derives from brucite, $Mg(OH)_2$, which consists of two-dimensional layered structure with cation substitution resulting in the ideal formula of $[M^{II}_{1-x}M^{III}_{x}(OH)_2]^{+}x[A^{-x/m}_{m}\cdot nH_2O]$ where trivalent cations replaces partially the divalent metal cations. The positive layer charge is balanced with anions in the interlayer space residing with water molecules. LDH type material is extensively studied as polymer filler and fire retardant because of its associated form factor, tunable composition, and its container role.[20–24] However, due to rather high charge densities, LDH platelets are not easy to exfoliate in contrast to swelling cationic clays bearing less layer charges. Stacked LDH platelets can be disassembled using chemical procedures such as those using environmental unfriendly and/or harmful solvent as shown using surfactant modified[25–28] and nitrate[29–31]

Additional Supporting Information may be found in the online version of this article.

© 2012 Wiley Periodicals, Inc.

comprising LDH platelets. For the latter, the delamination of large LDH crystals was associated to gradual platelets dissolution. One should also mention alkoxide[32] and lactate[33–34] intercalated LDH platelets that are delaminated in water at room temperature to form stable translucent colloidal solutions.

As far as LDH platelets dispersion into polyester is concerned, effective exfoliation of organo-modified LDH platelets was observed using either solution casting or melt extrusion as was illustrated for poly(ε-caprolactone) (PCL),[35] polylactic acid (PLA),[36–39] polyethylene terephthalate (PET)[40], and poly(3-hydroxybutyrate) (PHB)[41] resulting in corrugated and randomly dispersed layers. High-energy ball milling[42,43] as well as reflux conditions using cyclohexanone were also reported for PCL.[44]

To our knowledge a simple, room temperature and reproducible method free of organic intercalated anions and precarious solvents has not yet been reported for the exfoliation of LDH platelets into a waterborne polyester dispersion, thus yielding exfoliated polymer nanocomposite highly suitable for barrier properties relevant in polymer science.

Within this article a straightforward process to obtain exfoliated LDH polyester nanocomposite system enabling tunable filler loading is reported starting from a concentrated LDH phase solution. In addition, even if the polymer nanocomposite structures are well characterized, the intermediate transient compositions and time intervals were more arbitrarily chosen. Therefore, the progressive polymer diffusion into the filler host structure was recorded over time by following the evolution of X-ray diffraction and small angle X-ray scattering signals as well as by taking corresponding electron microscopic pictures.

EXPERIMENTAL

Materials

$Zn(NO_3)_2{\cdot}5H_2O$ (Acros, 98%), $Al(NO_3)_3{\cdot}9H_2O$ (Acros, 99%), NaOH (Acros, 97%), $NaNO_3$ (Acros, 99%), ethanol (Acros, 99%), and polyester (BASF Coatings, GmbH, 60 wt % solution) were used as received. The hydrotalcite-like materials were prepared by the coprecipitation method adapted from Miyata pioneer work.[45,46] Experimentally, 100 mL of a solution of the salts Zn^{2+} (0.1 mol) and Al^{3+} (0.05 mmol) were added dropwise to a solution containing $NaNO_3$ (0.05 mmol) under nitrogen atmosphere at constant pH of 8. The product was kept after centrifugation as slurry, and its associated solid content was measured by mass balance. Adopting the expected molecular weight formula of $Zn_2Al(OH)_6NO_3{\cdot}2H_2O$, LDH total mass yield of 93.6% was obtained from the initial reactant input, and the solid mass content of 17.1% was measured for slurry after 20 min centrifugation at 4000 rpm and drying at 30°C. The pH values of the further diluted slurries was measured to be in the range of pH = 6 to 10.

Polyester PES_h was obtained from a hydroxyl terminated polyester precursor, which is the polycondensation product of a mixture of dimerized fatty acid (PRIPOL 1012, Unichema), hydrogenated phthalic acid, hexamethylenediol, and 2,2-dimethyl-1,3-propanediol. This was chain extended using trimellitic acid anhydride. The PES functionality in terms of carboxylic acid (=AN) and hydroxyl groups (=OHN) expressed as the equivalents of mg KOH per gram solid polymer were 32 and 57, respectively, the mean molecular weight M_w being 30,000 with a PDI (M_w/M_n) of 10, determined with SEC using PMMA standards. The mass fraction of the dimerized fatty acid derived hydrocarbon increments (aliphatic and alicyclic CH, CH_2 moieties) within the PES_h polymer was calculated as 20 wt % and the polymer functionality in *N, N*-Dimethylethanolamine neutralized carboxylic acid groups was determined as 0.53 mmol/g. PES_h was used as a 60 wt % solution in a 1 : 1 part by weight mixture of water and 2-butoxyethanol.

Sample Preparation

The dispersion of LDH into polymer was conducted using different amounts of water and polymer. LDH slurry (17.1% solid content) was added in amounts to achieve the desired ratios filler to polymer taking into account both the solid content of the LDH slurry and the polyester concentration, the latter being used after dilution to 25.7% with deionized water in order to decrease the viscosity. The mixture was mechanically stirred at 130 rpm in air for various time periods. Previous experiments were carried out to study the stability of the polymer at the pH values in the range of 5–11 (the PES solutions being adjusted by the addition of "acid" and/or "base") in the time frame of weeks by following the acid number (AN) and the molecular weight distribution (SEC) in order to exclude that the PES hydrolyzes in the course of the sample preparation. Mass ratios between LDH and PES (LDH : PES) are given from 1 : 1 down to 1 : 9.

CHARACTERIZATION

Powder X-ray diffraction profiles (PXRD) were obtained with a Siemens D501 X-ray diffractometer using a diffracted beam monochromator Cu K source. Typical measurement conditions were in the 2θ-range 2°–70°, step size 0.04°(2), and step counting time 4 s. More specifically low angle measurements were performed closing the slits from 1° to 0.3° in the 2θ-range 1° or 0.7 to 10° with a step size 0.005°, and step counting time of 20 s. The instrumental full width at half maximum (FWHM) $\Delta\theta_0$ was measured with the silicon diffraction line (111) at $2\theta = 28.478°$, $\Delta\theta_0 = 0.154°$.

Fourier transform infrared (FTIR) spectra were recorded on a Perkin-Elmer 2000 FT spectrometer employing the KBr pellet technique.

Small-angle X-ray scattering (SAXS) and wide-angle X-ray scattering (WAXS) patterns were recorded on an Anton-Paar SAXSess mc^2 diffractometer using line collimation and Cu-Kα radiation. The distance between sample and detector was 261.2 mm. One should mention that contrary to PXRD SAXS/WAXS experiments were carried out on the original, liquid polymer-LDH composite slurries.

Transmission electron microscopy (TEM) images were recorded using a H7650 Hitachi microscope equipped with a camera AMT Hamamatsu. For the analysis, viscous slurries of polyester LDH nanocomposite were slightly dispersed into ethanol and deposited on Cu mesh, acceleration voltage was of 80 kV.

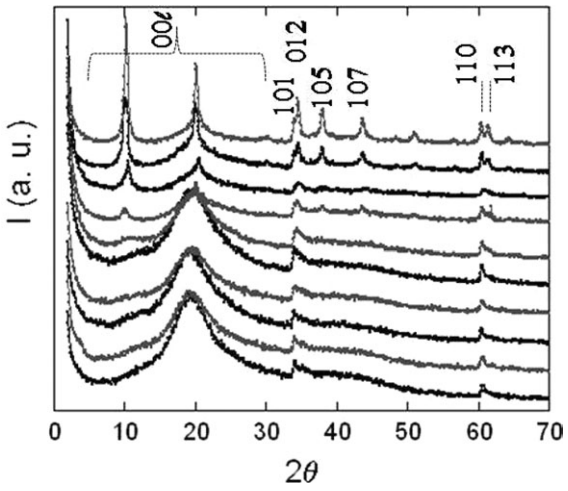

Figure 1. Stacked XRD of the dispersion of LDH into PESh using different LDH to polymer ratio, from top to bottom diagram 1 : 1 to 1 : 10 every 1 : *n*th.

RESULTS AND DISCUSSION

XRD Study

Staked powder diffraction patterns as a function of the relative amount of polyester against LDH filler displayed in Figure 1 show interesting changes. At a relative dispersion of 1 to 1, the diffraction lines are consistent with Zn_2Al/nitrate LDH structure.[29] As commonly described in R-3m space group in rhombohedral symmetry, the harmonic peaks (00ℓ) are present as well as some peaks (hkℓ) as identified in Figure 1. As expected the peak (110) independent of ℓ Miller index is evidently not influenced by the LDH sheet spacing, i.e. of the exfoliation process. This (110) peak position informs on the intralayer cation substitution and is related to the cell parameter *a*.

The presence of the ℓ –dependent diffraction lines specifically of lines (00ℓ) is indicating that the dispersion is not efficient and that the layered LDH structure remains intact thus resulting in a nonmiscible nanocomposite. When the relative amount of polymer increases, the diffraction lines (00ℓ) of LDH nitrate phase disappear progressively. One should note that two overlaying effects have to be considered to explain the loss of peak intensity related to the inorganic framework crystallinity: a possible disassembling effect due to platelets exfoliation and the dilution of crystallized objects within the polymer medium. Even if one cannot discard the dilution effect, the persistence of the (110) diffraction line even for the most diluted samples proves that the number of platelets is sufficient to diffract.

All the diffraction lines are not behaving similarly. The intralayer brucitic arrangement remains constant as can be seen with the diffraction line at $2\theta = 61°$ (110) whereas the hump centered around 35° stemming from the diffraction lines (101) and (012) becomes distorted because the latter peaks merges into the former with an increasing basal spacing and an increase in the turbostratic disorder. Conversely the diffraction lines (10ℓ and 11ℓ), highly dependent of the ℓ index, such as (105), (107), and (113) disappear due to an increase in the stacking distance (up to complete exfoliation) associated with an increase in the turbostratic disorder.

At the first glance, an exfoliated structure is reached for a ratio polymer to LDH of five for which exclusively the 10ℓ and 11ℓ reflections were observed. The quantitative exfoliation of the nitrate LDH phase (>50 g L^{-1}) in this case is much higher as compared to what was hitherto reported using nitrate intercalated or even surfactant modified LDH platelets[25–30] and compares quite well with recently published routes that rely on hexamine hydrolysis along with formamide[47] or which are based on the action of DMSO and ethylene-vinyl alcohol copolymer (EVOH).[48]

SAXS Study

Information on larger correlation distances obtained from SAXS spectroscopy is displayed in Figure 2. For a ratio 1 to 1, the scattering lines at $q = 7.001$ and 14.16 nm^{-1} are characteristic of the nitrate LDH phase and represent the lines (003) and (006), respectively (WAXS data are supplied in Supporting Information). At lower *q*-values, some humps are visible at values

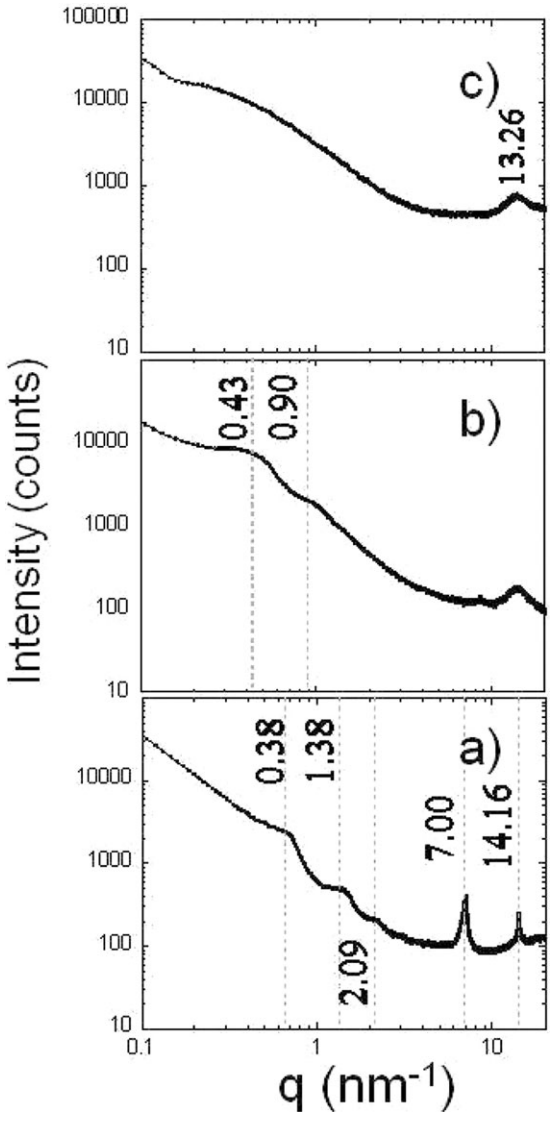

Figure 2. SAXS of the dispersion of LDH into PESh using (a) 1 : 1, (b) 1 : 5, and (c) 1 : 9 LDH to polymer ratio.

Applied Polymer SCIENCE

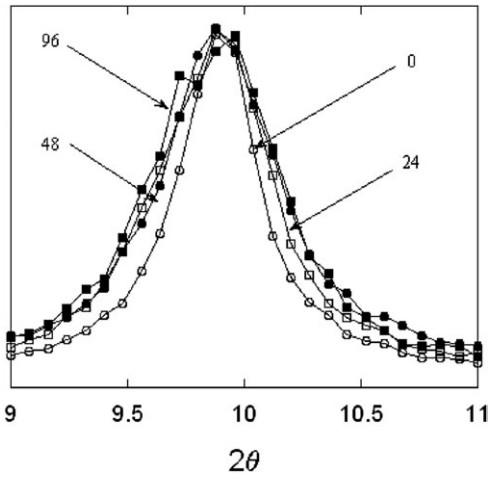

Figure 3. Enlarged XRD for LDH PESh dispersion using 1: 1 LDH to polymer ratio and after a storage time indicated in hours.

of 0.63, 1.38, and 2.09 nm^{-1} [materialized by dashed lines in Figure 2(c)] and corresponding to correlation distance values of 9.91, 4.53, and 3.01 nm, respectively. Such contrast corresponds to a stacking structure lines (00ℓ) with ℓ in the order of 1, 2, and 3, thus resulting in an intercalated polymer nanocomposite structure of about 10 nm. When increasing the polymer ratio to 1 : 5 (LDH : polymer), peaks due to nitrate LDH phase are then absent and only two large humps are observed at $q = 0.90$ and 0.43 nm^{-1}, resulting in distance of 7.1 and 14.4 nm. Once again this is indicative of an intercalated polymer nanocomposite structure of about 14 nm. Note that the scattering hump centered at $q = 13.26$ nm^{-1} is due to the polyester ($d = 0.47$ nm, $2\theta = 18.9°$). For a ratio of 1 to 9, there is neither peak nor hump observed other than the latter polymer contribution, thus informing of the total exfoliation of the LDH platelets in the low q-scale (up to 60 nm in distance scale). Again the observed hump at $q \approx 24$ nm^{-1} ($d = 0.26$ nm, $2\theta = 34°$) is characteristic of the merged lines (101) and (012) of LDH inside-sheet structure, and typical of the 10 two-dimensional reflection (Supporting Information).

The slope log I versus log q fitted by a power law dependence informs on the apparent mass fractal dimension of the scattering LDH platelets dispersed into the polymer. Indeed in reciprocal space, mass-fractal objects follow the power-law relationship in a log–log axes curve fitting profile:

$$I(q) \sim q^{-D_f}, \quad 1 \leq D_f \leq 3$$

and a slope of 2 is expected for a disk or sheet-like object.[49–51] A slope of 1.87, 1.71, and 1.44 in q domain 0.3–2 nm^{-1} is obtained for 1 : 1, 1 : 5 and 1 : 9 LDH to polymer dispersion, respectively. The deviation from the ideal value of 2 increases with the extent of exfoliation. This is counter-intuitive since a better exfoliation conceptually is associated with platelet-like particles. Such a deviation from the Euclidian object $D_f = 2$ could however be explained by the presence of fractal structures related to the interphase constituted by the polymer chains attached to the exfoliated platelets.

If increasing amounts of exfoliation is related to increasing dimensions of the intercalated species primary particles become more and more exposed and the resulting electron contrast with the polymer comprising aqueous continuous phase accentuates both the form factor of the tactoids but also an associated interphase roughness related to tethered polymer chains.

Exfoliation Time Dependence

To get some insights into the time dependence of the LDH dispersion within the polymer, XRD analysis is conducted after different times (Supporting Information). Qualitatively, one notes that there are some apparent changes in the stacked XRD diagrams that are depicted by an increase in the (00l) diffraction lines width as illustrated in the enlarged 2θ domain for the ratio LDH : PES of 1 : 1 (Figure 3). The width is related to the associated coherence length by the Scherrer relation:

$$L = \frac{0.9 * \lambda}{\Delta\theta_m^2 - \Delta\theta_0^2} * \frac{1}{\cos\theta}$$

where $\Delta\theta_m^2$ is the FWHM of the diffraction line, $\Delta\theta_0^2$ the instrumental FWHM (see Experimental section) and λ the wavelength. The difference of coherence length between two samples is then given by:

$$\frac{L_1}{L_2} = \frac{\sqrt{\Delta\theta_{m2}^2 - \Delta\theta_0^2}}{\sqrt{\Delta\theta_{m1}^2 - \Delta\theta_0^2}}$$

Between $t = 0$ and 96 h, FWHM of (003) is increased, and inversely the coherence length L is decreased from ≈20 nm down to 12 nm corresponding to the stacking of 22 and 14 platelets, respectively. Thus the lost approximately one-third of the initial platelets corresponds to the formation of intercalated polymer structure, which was observed by SAXS (Figure 2).

Time-evolution is even more pronounced on a dilute LDH sample, small angle scattering PXRD of the 1 : 9 dispersion being drastically modified (Figure 4). Starting initially from three correlated diffraction lines at $2\theta = 2.2$, 4.0, and 6.3° (basal spacing

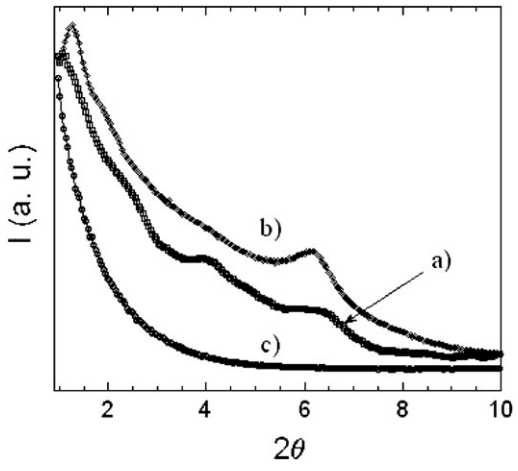

Figure 4. Low-angle XRD of LDH PESh dispersion using 1 : 9 LDH to polymer ratio and after a storage time of (a) 0, (b) 48, and (c) 96 h.

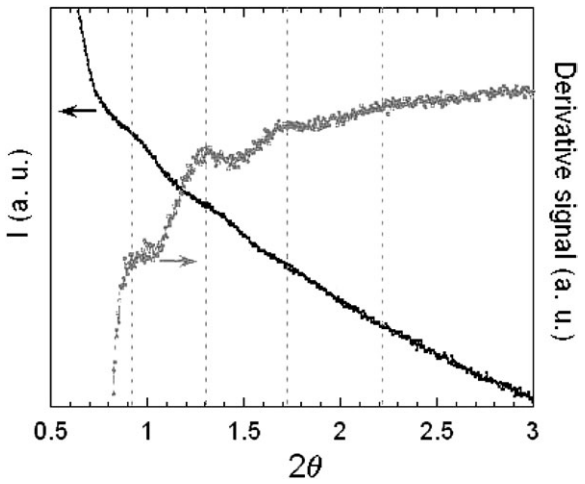

Figure 5. Low-angle XRD of LDH PESh dispersion stored 14 months using 1 : 5 LDH to polymer ratio.

of about 4 nm), the intercalated polymer nanocomposites interstitial spacing is shifted to 7.2 nm ($2\theta = 1.2°$) after 96 h and disappears after one month giving rise to the LDH platelets complete exfoliation, this in agreement with the previous SAXS data recorded after a long storage time.

To know whether the observed polymer nanocomposite structure largely intercalated such as the 1 : 5 dispersion ($d = 14.4$ nm) has reached a stabilized state after six month, small angle PXRD is conducted after more than one year (about 14 months). A layered structure is still observed with correlated lines at 0.9°, 1.3°, 1.8°, and 2.2° corresponding to spacings of 9.8, 6.8, 5.2, and 4.0 nm, respectively (Figure 5). The line positions are better visualized by the signals derivative. The associated distances can only be explained with a total inter-layer spacing of 20 nm, the first harmonic expected at $2\theta = 0.44°$, which is not accessible with the instrument being used. This demonstrates that the 14.4 nm intercalated structure after six months is still expanding to larger interlayer distance with a number of platelets barely sufficient to diffract. However, this resulting polymer nanocomposite structure maybe considered as exfoliated.

Infrared Analysis

To characterize the mutual effect arising from the dispersion as a function of the ratio LDH to polyester, FTIR is displayed in two selected wave number regions (Figure 6). One should note that FTIR spectra are not time dependent (performed on aged powders after drying). The presence of LDH platelets is observed in the low wave number region between 750 and 400 cm^{-1} where the inorganic metal framework stretching modes are expected. Two polymer vibration bands located at 1372 and 1725 cm^{-1} are apparently shifted to higher wave numbers to 1384 and 1733 cm^{-1}, respectively. However, for the LDH composite the former peak appears as a shoulder of the dominating sharp nitrate vibration band. The peak around 1730 cm^{-1} is characteristic for the carboxylic acid ester stretching vibration. In addition a slight shift to higher wavenumbers is observed for the vibration at 1240 cm^{-1} characteristic for trimellitic acid ester as well as for the vibration of C—H bonds at 1460 cm^{-1} characteristic for fatty acid bearing polyester. Note that the typical vibrations for CH and CH_2 of PES_h located around 2900 cm^{-1} are not modified as well as other vibrations located at 1065 and 1120 cm^{-1}, the latter being characteristic for hydrogenated phthalic acid ester. These observations show that the local environment of the trimellitic polymer acid ester functions is modified presumably due to the presence of LDH platelets, the carboxylate group of the trimellitic moiety acting as the charge balancing counter ion. The tethered polymer chains are most probably assembled in a dissimilar way as compared to the pristine PES as indicated by a shift of the peak at 1460 cm^{-1}, characteristic for C—H vibrations of aliphatic chains, to higher wavenumbers. Such a shift of IR peaks in the order of 8 cm^{-1} to higher wavenumbers because of a confinement of polymer chains has also been observed for the semicrystalline polyester PET.[52]

TEM Observations

TEM micrographs displayed in Figure 7 for the freshly prepared dispersion ratios 1 : 1, 1 : 5, and 1 : 9 picture the morphological

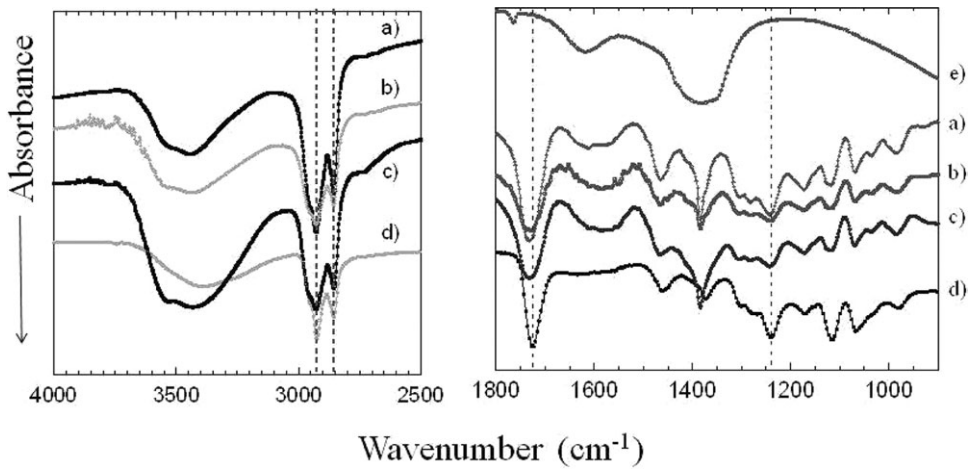

Figure 6. FTIR spectra of LDH PESh dispersion (a) 1 : 1, (b) 1 : 5, and (c) 1 : 9 LDH to polymer ratio using two selected wavenumber domains. PESh and LDH nitrate in (d) and (e).

dependence. Some stacked platelets are observed for the 1 : 1 dispersion, single platelets were not observed in that dispersion. For the other two dispersions, thin separated platelet structure presenting hexagonal feature is observed; however, the dispersion 1 : 5 exhibits some additional stacks of corrugated fringes. The isolated sheets were found to be instable, vanishing (degrading) rapidly under the electron beam. Additionally, the study of the morphological change against shell life of the slurries was attempted. However, the suspension started to be slightly gummy in time making difficult transmission microscopy analysis, the pictures were then very fuzzy and the solid particles blurred (not shown).

Masterbatch

The ability to exfoliate LDH platelets was also studied using successive dilution. Such a masterbatch approach is commonly used in polymer processing applications. Starting with a ratio of 1 to 1, the LDH proportion is then successively divided (Figure 8). The LDH nitrate phase present in the 1 : 1 masterbatch is progressively disappearing. An intercalated structure is observed for the ratio 1 : 7.5 with peaks at $2\theta = 6.2$ (1.43 nm) and 11.9° (0.93 nm) corresponding to a basal spacing of 2.8 nm. It is interesting to note the strong increase in intensity at small angles for 1 : 5 and 1 : 7.5 due to larger distance correlations, probably due to largely intercalated polymer nanocomposite structures while this rise in background intensity was not observed for 1 : 10. In-plane LDH structure related peaks are still observed for the highest dilution hence underlining the topotactic effect of PES chains diffusion as well as its associated turbostratic effect with the merging of the corresponding 10ℓ and 11ℓ two-dimensional reflections. This set of experiments demonstrates the potential to yield exfoliated composites by using a masterbatch technique.

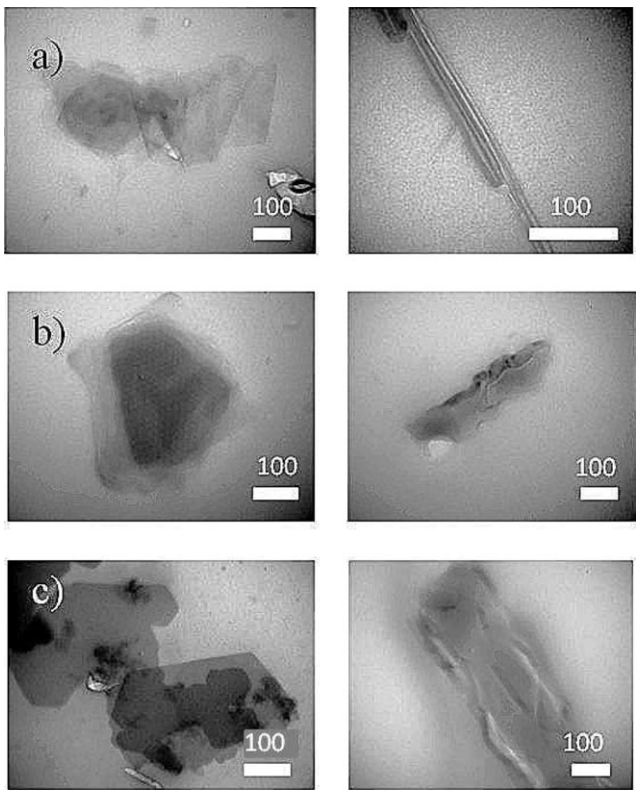

Figure 7. TEM of LDH PESh dispersion with (a) 1 : 1, (b) 1 : 5, and (c) 1 : 9 LDH to polymer ratio with view along the lateral size and along the stacking. Scale bar in nm.

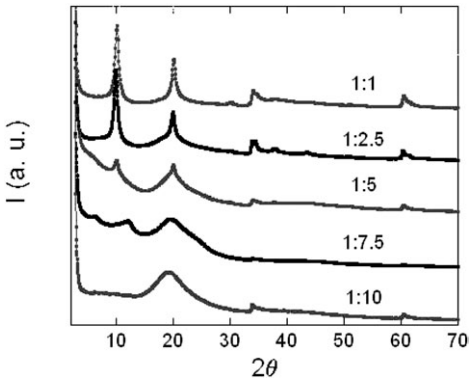

Figure 8. Stacked XRD of the dispersion of LDH into the polyester using successive freshly prepared dilutions as indicated by 1 : *n*, *n* being the polymer ratio. Scale bar in nm.

CONCLUSIONS

We demonstrate the possibility to achieve LDH platelets exfoliation through a simple procedure at room temperature using a waterborne polyester as a dispersing medium, this in the absence of organo-modification of the inorganic framework as usually performed using surfactant-type molecules. Since, the dispersion is carried out in air, it is remarkable to note that carbonate uptake is not observed even after prolonged storage.

The observed polymer nanocomposite structure is found to be either as coexisting phases, or as polymer intercalated as well as exfoliated platelets as a function of the dispersion ratio. Above a mass ratio PES_h to LDH of five, which corresponds to an equivalent ratio of the cationic layer charge to the carboxylic anions of one, a largely intercalated polymer structure with an interlayer spacing up to 20 nm was observed. This distance increases in time without any mechanical force applied, which underlines that the polymer chain diffusion into/between the LDH platelets is thermodynamically driven. Similarly exfoliation can as well be achieved by successive dilution yielding comparable results to those obtained from a one-step directed dilution.

Regarding the LDH inorganic platelets they may be considered as a filler that exfoliates yielding a polymer nanocomposite structure imparting barrier properties whereas the polymer may be perceived as a disassembling medium to achieve LDH sheets exfoliation.

It is the authors persuasion that such a smooth chemical modification approach to achieve exfoliation is of significant relevance for polymer processing related to applications that necessitate strength, toughness, as well as barrier properties. For the latter and particularly regarding stone chip resistance, the properties are now under investigation.

ACKNOWLEDGMENTS

The authors would like to thank H. Fitsch (BASF Coatings GmbH) for her discussion on IR study.

REFERENCES

1. Zang, Q. H.; Yu, A. B.; Lu, G. Q.; Paul, D. R. *J. Nanosci. Nanotechnol.* **2005,** *5*, 1574.
2. Utracki, L. A.; Sepehr, M.; Boccaleri, E. *Polym. Adv. Technol.* **2007,** *18*, 1.
3. Paul, D. R.; Robeson L. M. *Polymer* **2008,** *49*, 3187.
4. Duncan, T. V. *J. Colloid Interface Sci.* **2011,** *363*, 1.
5. Zhou, Q.; Verney, V.; Commereuc, S.; Chin, I.-J.; Leroux, F. *J. Colloid Interface Sci.* **2010,** *349*, 127.
6. Leroux, F.; Illaik, A.; Verney, V. *J. Colloid Interface Sci.* **2009,** *332*, 327.
7. Glampedaki, P.; Dutschk, V.; Jocic, D.; Warmoeskerken, M. C. G. *Biotechnol. J.* **2011,** *6*, 1219.
8. Djonlagic, J.; Nikolic, M. *RSC Green Chem. Series* **2011,** *12*, 149.
9. Katsarava, R.; Gomurashvili, Z. Handbook of Biodegradable Polymers; Wiley-VCH: Weinheim, **2011;** pp 107–131.
10. Rodriguez-Galan, A.; Franco, L.; Puiggali, J. *Polymer* **2011,** *3*, 65.
11. N. Supanchaiyamat, N.; Shuttleworth, P. S.; Hunt, A. J.; Clark, J. H.; Matharu, A. S. *Green Chem.* **2012,** *14*, 1759.
12. Ye, R.; Hayes, D. G. *Biocatal. Biotransform.* **2012,** *30*, 209.
13. Wu, W.; Zou, Y.; Chen, Y.; Li, J.; Lv, Z.; Wei, W.; Huang, T.; Liu, X. *Green Chem.* **2012,** *14*, 363.
14. Seungsoon, S. I.; Lee, W. In: Recent Advances in Polymer Nanocomposites: Synthesis and Characterisation: Polyester Nanocomposite; Thomas, S.; Zaikov, G. E.; Valsaraj, S. V., Eds.; V S P Inter Sciences, **2010;** p 233.
15. Raquez, J. M.; Nabar, Y.; Narayan, R.; Dubois, P. *J. Appl. Polym. Sci.* **2011,** *122*, 639.
16. Mahajan, S.; Barney, N. A. U.S. Pat. Appl. (**2010**), 20100331469 A1 20101230.
17. Hintze-Bruening, H.; Troutier-Thuilliez, A.-L.; Leroux, F. *Prog. Org. Coat.* **2009,** *64*, 193.
18. Hintze-Bruening, H.; Troutier, A. L.; Leroux, F. *Progr. Org. Coat.* **2011,** *70*, 240.
19. Troutier-Thuilliez, A.-L.; Hintze-Bruening, H.; Taviot-Guého, C.; Verney, V.; Leroux, F. *Soft Matter* **2011,** *7*, 4242.
20. Leroux, F.; Forano, C.; Prevot, V.; Taviot-Gueho, C. In: Encyclopia of Nanoscience and Nanotechnology: LDH Assemblies and Related Nanocomposites; Nalwa, H. S., Ed.; American Scientific Publishers: New York, **2009;** p 42.
21. Leroux, F.; Taviot-Guého, C. *J. Mater. Chem.* **2005,** *15*, 3628.
22. Pereira, C. M. C.; Herrero, M.; Labajos, F. M.; Marques, A. T.; Rives, V. *Polym. Degrad. Stab.* **2009,** *94*, 939.
23. Chiang, M. F.; Chu, M. Z.; Wu, T. M. *Polym. Degrad. Stab.* **2011,** *96*, 60.
24. Manzi-Nshuti, C.; Songtipya, P.; Manias, E.; Jimenez-Gasco, M. M.; Hossenlopp, J. M.; Wilkie, C. A. *Polymer* **2009,** *50*, 3564.
25. Leroux, F.; Adachi-Pagano, M.; Intissar, M.; Chauvière, S.; Forano, C.; Besse, J. P. *J. Mater. Chem.* **2000,** *11*, 105.
26. Venugopal, B. R.; Shivakumara, C.; Rajamathi, M. *J. Colloid Interface Sci.* **2006,** *294*, 234.
27. Jobbagy, M.; Regazzoni, A. E. *J. Colloid Interface Sci.* **2004,** *275*, 345.
28. Nakagaki, S.; Halma, M.; Bail, A.; Arizaga G.; Wypych, F. *J. Colloid Interface Sci.* **2005,** *281*, 417.
29. Liu, Z.; Ma, R.; Osada, M.; Iyi, N.; Ebina, Y.; Takada, K.; Sasaki, T. *J. Am. Chem. Soc.* **2006,** *128*, 4872.
30. Wu, Q.; Olafsen, A.; Vistad, O. B.; Roots, J.; Norby, P. *J. Mater. Chem.* **2005,** *15*, 4695.
31. Okamoto, K.; Sasaki, T.; Fujita, T.; Iyi, N. *J. Mater. Chem.* **2006,** *16*, 1608.
32. Gurski, J. A.; Blough, S. D.; Luna, C.; Gomez, C.; Luevano, A. N.; Gardner, E. A. *J. Am. Chem. Soc.* **2006,** *128*, 8376.
33. Hibino, T.; Kobayashi, M. *J. Mater. Chem.* **2005,** *15*, 653.
34. Jaubertie, C.; Holgado, M. J.; San Roman, M. S.; Rives, V. *Chem. Mater.* **2006,** *18*, 3114.
35. Mangiacapra, P.; Raimondo, M.; Tammaro, L.; Vittoria, V.; Malinconico, M.; Laurienzo, P. *Biomacromolecules* **2007,** *8*, 3147.
36. Mahboobeh, E.; Yunus, W. M. Z.; Hussein, Z.; Mansor, Z. A.; Azowa, I. N. *J. Appl. Polym. Sci.* **2010,** *118*, 1077.
37. Katiyar, V.; Gerds, N.; Koch, C. B.; Risbo, J.; Hansen, H. C. B.; Plackett, D. *J. Appl. Polym. Sci.* **2011,** *122*, 112.
38. Wang, D. Y.; Leuteritz, A.; Wang, Y. Z.; Wagenknecht, U.; Heinrich, G. *Polym. Degrad. Stab.* **2010,** *95*, 2474.
39. Pan, P. B.; Zhu, B.; Dong, T.; Inoue, Y. *J. Polym. Sci. B* **2008,** *46*, 2222.
40. Lee, W. D.; Im, S. S.; Lim, H.-M.; Kim, K.-J. *Polymer* **2006,** *47*, 1364.
41. Hsu, S.-F.; Wu, T.-M.; Liao, C.-S. *J. Polym. Sci. B* **2006,** *44*, 3337.
42. Bugatti, V.; Costantino, U.; Gorrasi, G.; Nocchetti, M.; Tammaro, L.; Vittoria, V. *Eur. Polym. J.* **2010,** *46*, 418.
43. Costantino, U.; Bugatti, V.; Gorrasi, G.; Montanari, F.; Nocchetti, M.; Tammaro, L.; Vittoria, V. *ACS Appl. Mater. Inter.* **2009,** *1*, 668.
44. Peng, H.; Han, Y.; Liu, T.; Tjiu, W. C.; He, C. *Thermochim. Acta* **2010,** *502*, 1.
45. Miyata, S. *Clays Clay Miner.* **1983,** *31*, 305.
46. Troutier-Thuilliez, A.-L.; Taviot-Guého, C.; Cellier, J.; Hintze-Bruening, H.; Leroux, F. *Prog. Org. Coat.* **2009,** *64*, 182.
47. Antonyraj, C. A.; Koilraj, P.; Kannan, S. *Chem. Commun.* **2010,** 46, 1902.
48. Zhao, Y.; Yang, W.; Xue, Y.; Wang, X.; Lin, T. *J. Mater. Chem.* **2011,** *21*, 4869.
49. Jouault, N.; Vallat, P.; Dalmas, F.; Said, S.; Jestin, J.; Boué, F. *Macromolecules* **2009,** *42*, 2031.
50. Bugnicourt, E.; Galy, J.; Gérard, J.-F.; Boué, F.; Barthel, H. *Polymer* **2007,** *48*, 949.
51. Schaefer, D. W.; Justice, R. S. *Macromolecules* **2007,** *40*, 8501.
52. Xiazhen, Y.; Fujin, L.; Deyan, S.; Renyan, Q. *Polymer* **1991,** *32*, 125.